

Manuscript Number:

Title: Towards effective small scale microbial fuel cells for energy generation from urine

Article Type: Research Paper

Keywords: Microbial Fuel Cell; Urine; Biochar; Bioenergy

Corresponding Author: Dr. Mirella Di Lorenzo,

Corresponding Author's Institution: University of Bath

First Author: Jon Chouler

Order of Authors: Jon Chouler; George A Padgett; Petra J Cameron; Kathrin Preuss; Maria-Magdalena Titirici; Ioannis Ieropoulos; Mirella Di Lorenzo

Abstract: To resolve an increasing global demand in energy, a source of sustainable and environmentally friendly energy is needed. Microbial fuel cells (MFC) hold great potential as a sustainable and green bioenergy conversion technology that uses waste as the feedstock.

This work pursues the development of an effective small-scale MFC for energy generation from urine. An innovative air-cathode miniature MFC was developed, and the effect of electrode length was investigated. Two different biomass derived catalysts were also studied. Doubling the electrode length resulted in the power density increasing by one order of magnitude (from 0.053 to 0.580 W m<sup>-3</sup>). When three devices were electrically connected in parallel, the power output was over 10 times higher compared to individual units. The use of biomass-derived oxygen reduction reaction catalysts at the cathode increased the power density generated by the MFC up to 1.95 W m<sup>-3</sup>, thus demonstrating the value of sustainable catalysts for cathodic reactions in MFCs.

Dr Mirella Di Lorenzo  
Department of Chemical Engineering  
University of Bath  
Bath  
BA2 7AY  
+44(0)1225 385574  
[M.di.Lorenzo@bath.ac.uk](mailto:M.di.Lorenzo@bath.ac.uk)

29<sup>th</sup> October 2015

Dear Editor,

It is our great pleasure to submit our manuscript titled '**Towards effective small scale microbial fuel cells for energy generation from urine**' to the Electrochimica Acta Journal.

Our work pursues the development of an effective small-scale MFC and the arrangement of multiple MFC units in stack for energy generation from urine.

The Microbial Fuel Cell (MFCs) is an extremely attractive technology that generates electricity from waste too-wet-to-be-burnt, such as wastewater, which otherwise require energy to be disposed of. In combination with other renewable technologies, MFCs can surely play an important role in addressing the triple challenge of finding technological solutions that support secure, affordable, and environmentally-sensitive energy.

Miniaturisation of the MFC technology and the arrangement of multiple units in stack is currently considered the most promising way to enhance the power output. The potentialities of this 'miniaturisation and multiplication' strategy, however, have not been fully explored yet.

In this context, our work reports the development of an innovative air-cathode miniature MFC; analyses the effect that the electrodes length has on performance; and investigates the optimal electrical configuration for the arrangement of multiple units in stack. To improve the efficiency of the MFC, the use of sustainable and cost-effective biomass-based carbon catalysts (biochar) for the oxygen reduction at the cathode was also tested.

Our work provides important guidelines on effective designs of miniature MFCs and arrangement in stack, which can help boosting the power generated by this technology.

Given the importance of our findings, we have targeted one of the top journals in the field for our manuscript. We believe that our exciting findings, very much in line with the objectives of the Electrochimica Acta Journal, are extremely timely and are of great interest to a wide range of researchers, especially in the field of biological fuel cells, and bioenergy.

Yours sincerely,

Dr Mirella Di Lorenzo (on behalf of all the authors)



## **Suggested Referees**

Prof Ian Head  
Newcastle University  
[ian.head@ncl.ac.uk](mailto:ian.head@ncl.ac.uk)

Prof Giuliano Premier  
University of South Wales  
[iano.premier@southwales.ac.uk](mailto:iano.premier@southwales.ac.uk)

Prof William Sloan  
University of Glasgow  
[William.Sloan@glasgow.ac.uk](mailto:William.Sloan@glasgow.ac.uk)

1  
2  
3 **Towards effective small scale microbial fuel cells for**  
4  
5  
6 **energy generation from urine**  
7  
8  
9

10  
11  
12  
13 Jon Chouler <sup>a,b</sup>, George A. Padgett <sup>a</sup>, Petra J. Cameron <sup>c</sup>, Kathrin Preuss <sup>d,e</sup>, Maria-Magdalena  
14  
15 Titirici <sup>d,e</sup>, Ioannis Ieropoulos <sup>f</sup>, Mirella Di Lorenzo <sup>b,\*</sup>  
16  
17  
18  
19  
20  
21

22 <sup>a</sup> University of Bath, Department of Chemical Engineering, Bath, BA2 7AY, UK;  
23  
24

25 <sup>b</sup> Centre for Sustainable Chemical Technologies, University of Bath, Bath BA2 7AY, UK  
26  
27

28 <sup>c</sup> University of Bath, Department of Chemistry, Bath, BA2 7AY, UK  
29  
30  
31

32 <sup>d</sup> Queen Mary University of London, School of Engineering and Materials Science, London,  
33  
34 E1 4NS, UK  
35  
36  
37

38 <sup>e</sup> Queen Mary University of London, Materials Research Institute, London, E1 4NS,UK  
39  
40

41 <sup>f</sup> Bristol BioEnergy Centre, Bristol Robotics Laboratory, University of the West of England,  
42  
43 Bristol, UK  
44  
45  
46  
47  
48  
49

50 \*Corresponding author:  
51  
52

53 Email: M.Di.Lorenzo@bath.ac.uk  
54  
55  
56

57 Telephone: +44(0)1225 385574  
58  
59  
60  
61  
62  
63  
64  
65

## Abstract

To resolve an increasing global demand in energy, a source of sustainable and environmentally friendly energy is needed. Microbial fuel cells (MFC) hold great potential as a sustainable and green bioenergy conversion technology that uses waste as the feedstock.

This work pursues the development of an effective small-scale MFC for energy generation from urine. An innovative air-cathode miniature MFC was developed, and the effect of electrode length was investigated. Two different biomass derived catalysts were also studied. Doubling the electrode length resulted in the power density increasing by one order of magnitude (from 0.053 to 0.580 W m<sup>-3</sup>). When three devices were electrically connected in parallel, the power output was over 10 times higher compared to individual units. The use of biomass-derived oxygen reduction reaction catalysts at the cathode increased the power density generated by the MFC up to 1.95 W m<sup>-3</sup>, thus demonstrating the value of sustainable catalysts for cathodic reactions in MFCs.

**Keywords:** Microbial Fuel Cell, Urine, Biochar, Bioenergy

# 1 Introduction

1  
2  
3 In the face of the growing problem of fossil fuel depletion, there is global interest in  
4  
5 developing sustainable and environmentally friendly forms of energy. One form of alternative  
6  
7 energy that may be viable in addressing this problem is bioenergy [1,2]. In this context,  
8  
9  
10 Microbial fuel cells (MFC) hold great potential as green and carbon-free technology that  
11  
12 directly converts biomass into electricity [3].  
13  
14

15  
16 MFCs are electrochemical devices that take advantage of the metabolic processes of  
17  
18 microorganisms to directly convert organic matter into electricity with high efficiencies for  
19  
20 long periods of time [4]. Compared to other bioenergy conversion processes (i.e. anaerobic  
21  
22 digestion, gasification, fermentation), MFCs have the advantage of reduced amounts of sludge  
23  
24 production [5], as well as cost-effective operation, since they operate under ambient  
25  
26 environmental conditions (temperature, pressure) [6]. Moreover, MFCs require no energy  
27  
28 input for aeration so long as the cathode is passively aerated, for example *via* the use of a  
29  
30 single-chamber device [7]. Lastly, MFCs have the ability to generate energy remotely by  
31  
32 using a range of feed stocks, and can thus be used in areas of poor energy infrastructure.  
33  
34  
35 Organic waste used as a feed stock in particular offers attractive prospects from its cost-  
36  
37 effectiveness and abundance. Urine has been demonstrated to be an effective feed stock for  
38  
39 MFC operation with the additional benefit of nitrogen, phosphate and potassium recovery  
40  
41 from the fuel [8].  
42  
43  
44  
45  
46  
47

48  
49 Despite the breadth of applications and the growing interest in MFC technology over the past  
50  
51 two decades, commercialisation of MFCs for energy generation has not yet been realised.  
52  
53

54  
55 The major limiting factors that hinder the practical implementation of MFCs at large scale,  
56  
57 are the cost of materials used and the difficulties in the scale-up process [9].  
58  
59  
60  
61  
62

1 Typically the electrodes are made from highly cost-effective materials such as carbon cloth,  
2 carbon paper, and graphite based rods, plates and granules. Recently, even some metals, such  
3 as copper and silver, have been shown to be effective anode materials [10]. However,  
4 expensive metals, such as platinum, are usually used at the cathode to enhance the oxygen  
5 reduction reaction (ORR) [11–13]. Recently, the use of biomass-derived catalysts recovered  
6 from waste has been proposed as an effective alternative to expensive metal ORR catalysts. In  
7 particular, biomass-derived materials from wood [14], sewage sludge [15] and bananas [16]  
8 have been shown to function as ORR catalysts to boost MFC performance whilst reducing the  
9 device cost and its carbon footprint. Doping these materials with heteroatoms such as nitrogen  
10 and sulphur [17], also in combination with nanoparticles like iron [18], has been shown to  
11 enhance the catalytic activity towards the ORR even further.  
12  
13  
14  
15  
16  
17  
18  
19  
20  
21  
22  
23  
24  
25  
26

27 Another limitation towards practical implementations of MFCs, is their poor performance due  
28 to high internal resistances and ohmic losses experienced upon scale-up [19]. Consequently,  
29 the power performance of MFCs is low compared to other renewable energy technologies  
30 [8,20]. Considering the thermodynamic limit of an MFC (1.14 V open circuit), the most  
31 feasible approach to scale-up the power generated by this technology is to create a collection  
32 of multiple MFCs connected together as a stack. By miniaturising individual MFC units,  
33 stacks of large numbers of constituent MFCs could be developed, within a compact footprint.  
34 This approach has been referred as the ‘miniaturisation and multiplication’ strategy [21].  
35  
36  
37  
38  
39  
40  
41  
42  
43  
44  
45

46 MFC miniaturisation offers other advantages as well. The large surface area-to-volume ratio  
47 and short electrode distances - typical characteristics of miniature MFCs- provide a pathway  
48 to reducing ohmic losses, improving the mass transport processes between bulk liquid,  
49 biofilm and electrode and therefore enhancing power performance [22]. The consolidation of  
50 microfabrication techniques has led to the first prototypes of micro-sized MFCs, which have  
51 been discussed in a recent review [9]. Nonetheless, the process of miniaturisation of the MFC  
52  
53  
54  
55  
56  
57  
58  
59  
60  
61  
62  
63  
64  
65

1 technology is still in its infancy. The two-chamber configuration is typically adopted for the  
2 miniature MFCs reported thus far, and, usually, a ferricyanide solution is used as the catholyte  
3 [23]. Given the greater operational simplicity and cost-effectiveness of oxygen diffusion  
4 systems, air-cathode MFC designs should be considered instead. Moreover, a more in-depth  
5 analysis on how to effectively miniaturise the system for better performance would be  
6 beneficial.  
7

8  
9  
10  
11  
12  
13  
14 With the aim of guiding the development of efficient small-scale MFCs, this study reports the  
15 development of an innovative air-cathode small-scale MFC and analyses the effect that the  
16 chamber length (and therefore the electrodes length) have on its performance either when  
17 operated as a single unit or when assembled in a stack. No expensive metals have been  
18 employed at the cathode, and the use of two types of innovative and highly sustainable  
19 biomass-derived ORR catalysts are compared with a catalyst-free device.  
20  
21  
22  
23  
24  
25  
26  
27  
28  
29  
30  
31

## 32 **2 Experimental**

### 33 *2.1 Materials*

34  
35  
36 All reagents used were of analytical grade and purchased from Sigma-Aldrich and Alfa Aesar.  
37  
38 Unless otherwise stated, all aqueous solutions used were prepared with reverse osmosis  
39 purified water. Polydimethylsiloxane (PDMS, Dow Corning Sylgard 184) was purchased  
40 from Ellsworth Adhesives (UK).  
41  
42  
43  
44  
45  
46  
47  
48

49  
50 Artificial Urine Medium (AUM) was used as the feedstock and prepared as previously  
51 described [24]. Tetrasodium pyrophosphate was added to the AUM as a precipitation  
52 inhibitor. The resulting feedstock was sterilised by filtration (Grade p8 filter paper, Fisher  
53 Scientific, UK) prior to use.  
54  
55  
56  
57  
58  
59  
60  
61  
62  
63  
64  
65



## 2.2 Microbial Fuel Cells

Two geometries were used in this study, leading to the fuel cells MFC\_S (for short length) and MFC\_L (for longer length). Both MFCs consisted of a single chamber made of a rectangular piece of PDMS and sandwiched between two Perspex plates (Figure 1). The channel mould was made of PA 2200 nylon plastic and purchased from Shapeways, New York, USA. The top plate had a square opening as large as the channel cross sectional area to host the cathode, which was opened to air. The anode was instead placed at the bottom of the channel. The two geometries considered differed from each other according to the length of the anode chamber. In particular, MFC\_S was characterised by a total anodic chamber volume of 64  $\mu\text{L}$  (length = 4 mm, width = 4 mm, height = 4 mm), while MFC\_L had an anodic volume of 128  $\mu\text{L}$  (MFC\_L: length = 8 mm, height = 4mm, width = 4mm).

The anode and cathode (geometric surface area = 16  $\text{mm}^2$  for the case of MFC\_S, and 32  $\text{mm}^2$  for MFC\_L) were made of carbon cloth (untreated carbon cloth type-B, E-Tek, USA) and threaded with titanium wire (Advent Research Materials, Oxford, UK) for electrical contact. The proton exchange membrane (Nafion® 115, Sigma-Aldrich) was hot pressed to the cathode by applying a pressure of approximately 2.5 bar for 12 minutes at a temperature of 150 °C.

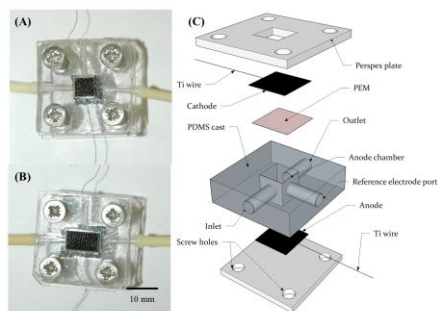


**Figure 1.** MFCs used in this study; A: Photograph of MFC\_S; B: Photograph of MFC\_L; C: Schematic layout of the device.

### 2.3 Use of a biomass-derived oxygen reduction reaction catalyst

Two different biomass-derived ORR catalysts, named as BC1 and BC2, produced by hydrothermal carbonisation, were tested at the cathode of MFC\_L. Both catalysts were synthesised from glucose and ovalbumin as described in [25] and [17]. BC1 is a nitrogen doped carbon aerogel, while BC2 is a nitrogen and sulphur co-doped aerogel that was prepared with an additional iron source. A loading of 1.5 mg per cm<sup>2</sup> of the cathode area was used for each ORR catalyst. 1.5 mg of catalyst was mixed with 105 µL of Nafion® perfluorinated resin solution and sonicated for 3 minutes. The resulting suspension was spread over 1 cm<sup>2</sup> of carbon cloth. Once dried, the doped cathode was bound to the Nafion® membrane as shown in Figure 1 above. The MFCs with the doped cathodes were named as MFC\_BC1 and MFC\_BC2, according to the ORR catalyst used.

The morphology of the resulting electrodes was characterised using a Hitachi S-4300 scanning electron microscope (SEM).

### 2.4 Operation of the MFCs

All MFCs were fed with AUM at the flow rate of 0.36 mL min<sup>-1</sup> (hydraulic residence times of 11 seconds and 22 seconds for MFC\_S and MFC\_L respectively). The cells were connected to a multi-channel peristaltic pump (Ecoline, Ismatech, Germany) via Pharmed® BPT tubing, ID 1.6 mm (Cole-Parmer, UK). The anode and cathode were connected to a voltmeter (ADC-

1  
2  
3  
4  
5  
6  
7  
8  
9  
10  
11  
12  
13  
14  
15  
16  
17  
18  
19  
20  
21  
22  
23  
24  
25  
26  
27  
28  
29  
30  
31  
32  
33  
34  
35  
36  
37  
38  
39  
40  
41  
42  
43  
44  
45  
46  
47  
48  
49  
50  
51  
52  
53  
54  
55  
56  
57  
58  
59  
60  
61  
62  
63  
64  
65

24 Pico data logger, Pico Technology, UK) and to an external load to polarise the cell and monitor the cell potential under closed circuit conditions.

Maturing of the electrochemically active bacteria (enrichment) at the anode was performed over a period of five days. It consisted of feeding the MFCs under continuous recirculation conditions with AUM containing 1% v/v mixed culture of bacteria (anaerobic sludge provided by Wessex Water, Scientific Laboratory in Salford, UK), which was replaced on a daily basis. The fuel cells were first operated under open circuit conditions for up to 2 hours, and then connected to an external load of 1 k $\Omega$ . After the enrichment, the MFCs were fed continuously with AUM and no bacteria.

Polarisation experiments were performed by connecting the MFCs to a series of external loads, varying from 10  $\Omega$  to 1000 k $\Omega$ , controlled by an external variable resistor (RS-200 Resistance substitute, IET Labs Inc., USA), and by measuring the pseudo steady state output potential after 20 minutes. Before the test, the MFC was left under open circuit for no more than 2 hours to allow a steady state open circuit voltage (OCV) to develop. Ohm's law was used to determine the corresponding current ( $I$ ) at each external load value ( $I = V/R$ , where  $V$ , and  $R$  are voltage and resistance respectively). The power ( $P$ ) was calculated by using Joule's law ( $P = I^2/R$ ). Power density was calculated by dividing the power by the MFC chamber volume, while current density was calculated by dividing the current by the total macro surface area of the anode.

The internal resistance ( $R_{int}$ ) of the MFC was calculated from the linear fit of the ohmic region of each polarisation cell potential curve ( $R_{int} = \Delta V/\Delta I$ ), as previously described [3].

## 2.5 Stacking

To scale-up the power output, MFC units with the same geometry were electrically stacked in series and in parallel, as shown in Figure 2. The MFCs were enriched individually and stacked after the five days of enrichment, once a steady current was generated. Once stacked, the MFC units were fed in parallel with AUM and no bacteria. The polarisation experiments on the stack were performed after at least 24 hours of operation.

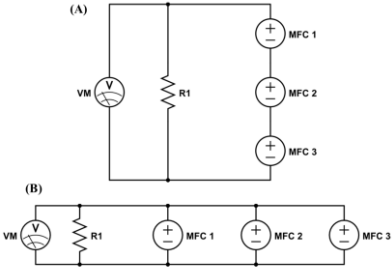


**Figure 2.** Schematic for electrical stacking MFC units in series (A) and in parallel (B): R1 = external load, VM = voltmeter.

2.6 Calculations

The maximum current density ( $I_{max}$ ) under mass transport limiting conditions at the electrode, is expressed according to [26] as:

$$I_{max} = nFD \frac{\Delta C}{\lambda} \tag{1}$$

Where  $n$  is number of electrons equivalent corresponding to the limiting compound (substrate),  $F$  is Faraday’s constant ( $96485 \text{ C mol}^{-1}$ ),  $D$  is the normalised diffusivity of the limiting compound (substrate) ( $\text{m}^2 \text{ s}^{-1}$ ),  $\Delta C$  is the concentration gradient of the limiting compound ( $\text{mol m}^{-3}$ ), and  $\lambda$  is the diffusion layer thickness (m).

1  
2  
3  
4  
5  
6  
7  
8  
9  
10  
11  
12  
13  
14  
15  
16  
17  
18  
19  
20  
21  
22  
23  
24  
25  
26  
27  
28  
29  
30  
31  
32  
33  
34  
35  
36  
37  
38  
39  
40  
41  
42  
43  
44  
45  
46  
47  
48  
49  
50  
51  
52  
53  
54  
55  
56  
57  
58  
59  
60  
61  
62  
63  
64  
65

The Reynold's number ( $Re$ ) and mass transfer coefficient ( $k_c$ ) for laminar flow in a channel is defined as [27]:

$$Re = \frac{\rho v d_H}{\mu} \quad (2)$$

$$k_c = 0.664(Re)^{1/2} \left( \frac{\mu}{\rho D} \right)^{1/3} \left( \frac{D}{H} \right) \quad (3)$$

Where  $\rho$  is specific density of the fluid ( $\text{kg m}^{-3}$ ),  $v$  is the linear velocity of the fluid ( $\text{m s}^{-1}$ ),  $d_H$  is the hydraulic diameter of the flow channel (m), and  $\mu$  is the viscosity of the fluid ( $\text{kg m}^{-1} \text{s}^{-1}$ ).

The hydraulic diameter of the channel ( $d_H$ ) is related to the channel length according to Equation 4:

$$d_H = \frac{4(LH)}{2(L + H)} \quad (4)$$

Where  $H$  is the height (m), and  $L$  is the lateral dimension length (m).

The diffusion-layer thickness ( $\lambda$ ) at the electrode surface was calculated with the following equation:

$$\lambda = \frac{D}{k_c} \quad (5)$$

### 3 Results and Discussion

#### 3.1 Effect of Electrode Length on Performance

1 The influence of the electrode length on the performance of small scale MFCs, was  
2 investigated in this study by operating two different fuel cells geometries, MFC\_S and  
3 MFC\_L, characterised by the same cross sectional area (and therefore the same electrode  
4 spacing, 4 mm) but different channel lengths. In particular, the length of the anodic chamber  
5 in MFC\_L was two times larger than MFC\_S. The resulting performances are compared in  
6 terms of the power and cell polarisation curves, produced from the polarisation experiment, as  
7 shown in Figure 3.  
8  
9

10 The OCV for MFC\_S and MFC\_L were  $253 \pm 86$  mV and  $312 \pm 59$  mV respectively. High  
11 internal resistances were observed for both devices. In particular, MFC\_L showed an internal  
12 resistance of 33 k $\Omega$ , which is comparable to the values of miniature MFCs reported in the  
13 literature [28,29]. The internal resistance of MFC\_S was higher at 242 k $\Omega$ . From the cell  
14 polarisation curves in Figure 3, ohmic losses appear to be dominating in both MFC\_S and  
15 MFC\_L, suggesting that the electrical resistances of the electrodes, membrane and electrolyte  
16 are mostly responsible for the internal resistance of the MFC. Accordingly, there is little  
17 evidence of mass transfer limitations taking place in the MFC, which may be a result of  
18 miniaturisation, which, as expected, allows good transfer of substrate from the bulk fluid to  
19 the biofilm on the anode [30].  
20  
21  
22  
23  
24  
25  
26  
27  
28  
29  
30  
31  
32  
33  
34  
35  
36  
37  
38  
39  
40  
41  
42  
43  
44  
45  
46  
47  
48  
49  
50  
51  
52  
53  
54  
55  
56  
57  
58  
59  
60  
61  
62  
63  
64  
65

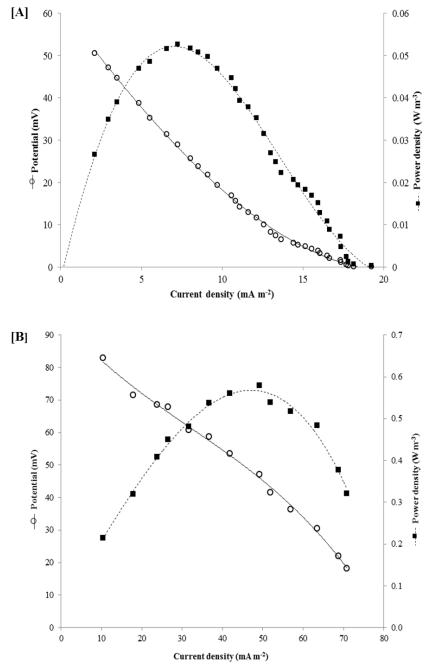


**Figure 3.** Power and polarisation curves. A: MFC\_S; B: MFC\_L. Current density refers to the anode surface area: MFC\_S = 16 mm<sup>2</sup>; MFC\_L = 32 mm<sup>2</sup>. Volumetric power density refers to the MFC chamber volume: MFC\_S = 64  $\mu$ L; MFC\_L = 128  $\mu$ L. For each geometry, data is the average of 3 devices, with up to 22% error.

Doubling the length of the anode chamber improved the power density by a factor of 11. The maximum power densities of MFC\_S and MFC\_L were 0.053 and 0.580 W m<sup>-3</sup> respectively, and the current densities at the maximum power output were 7.3 and 49.1 mA m<sup>-2</sup> respectively.

The increase in power and current density is suspected to be due to an increase in the mass transfer between the bulk fluid, biofilm and electrode surface. When observing the cross section of a MFC square electrode chamber, the height,  $H$ , and the lateral dimension (length),  $L$ , will affect the performance of the device. On one hand, when the height of the channel is reduced (i.e. the distance between electrodes is reduced) in the MFC, the miniaturised device

benefits from a greater rate of mass transfer due to an increase in the surface area to volume ratio of the device [22]. As a result, the power density generated by miniature MFCs is higher than large-scale devices [31]. On the other hand, when the lateral dimension of the channel (length),  $L$ , of the electrode chamber is increased, the hydraulic diameter of the channel is increased as per Equation 4. Consequently, the mass transfer coefficient,  $k_C$ , will increase as per Equations 2 and 3. Therefore, when  $L$  is increased, whilst maintaining a fixed  $H$ , the mass transfer coefficient is increased, and hence the diffusion-layer thickness at the electrode surface will decrease (Equation 5). By altering the length of the channel, the maximum current density available at the electrode will therefore increase (Equation 1), and, consequently, result in high fuel consumption efficiency and an improvement in power performance.

Figure 4 demonstrates that increasing the length of the flow channel, for a fixed flow rate, will increase the mass transfer coefficient and decrease the diffusion-layer thickness. Values here have been calculated using Equations 1-5, with the flow rate at  $0.36 \text{ mL min}^{-1}$ , and a linear velocity of  $22.5 \text{ mm min}^{-1}$ . For urine, the kinematic viscosity ( $\mu / \rho$ ) is estimated to be  $1.07 \text{ mm}^2 \text{ s}^{-1}$  at  $20 \text{ }^\circ\text{C}$  [32], and the diffusivity of urea in water is  $0.082 \text{ mm}^2 \text{ min}^{-1}$  [33].

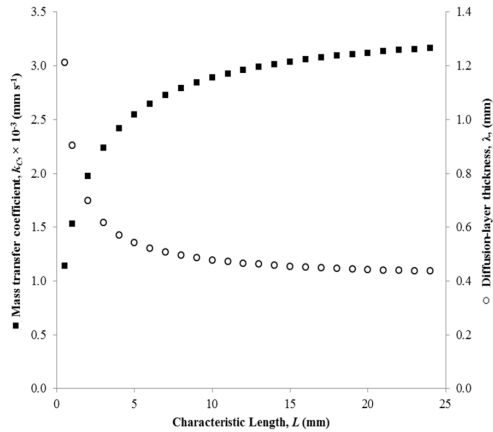


**Figure 4.** Effect of length of MFC channel on mass transfer coefficient and diffusion-layer thickness moving from 0.5 to 25 mm. Values plotted are for a flow rate of  $0.36 \text{ mL min}^{-1}$ .



1  
2  
3 To ensure that these assumptions are valid, the flow regime in the flow channel must be  
4  
5 laminar. This is confirmed by the  $Re$  values for MFC\_S and MFC\_L, which are 1.4 and 1.9  
6  
7 respectively, as calculated by considering  $L$  values of 4 and 8 mm, for MFC\_S and MFC\_L  
8  
9 respectively, and  $H$  equal to 4 mm.  
10

11  
12  
13 By increasing the length of the electrode in the MFC devices, a better fuel efficiency has been  
14  
15 achieved, with consequent improvement in performance [34]. This is in accordance with a  
16  
17 recent study by [35] whereby increasing the length of a graphite fibre brush anode from 12  
18  
19 mm to 30 mm the power density increased from 1.13 to 1.65 W m<sup>-2</sup>.  
20  
21  
22  
23  
24  
25  
26

### 27 3.2 *Stacking the Miniature MFCs*

28  
29  
30

31 To scale up the power output, MFC\_S and MFC\_L were arranged in stacks of three units  
32  
33 each. The MFC\_S units were electrically connected either in parallel or in series to evaluate  
34  
35 the best configuration.  
36  
37  
38

39 Figure 5A reports the results from the polarisation experiments. The maximum power output  
40  
41 increased almost 4 times when the MFC\_S units operated as a series stack compared to  
42  
43 individual units, while when stacked in parallel the power output was 14 times higher. This  
44  
45 result is in agreement with previous studies that report voltage reversal effects when the  
46  
47 MFCs are arranged in series [36]. The reversal in some of the cells in the series stack is  
48  
49 caused by the unavoidable increase in the internal resistances of the MFC units operated in  
50  
51 series, as previously reported [36,37]. Thereby, power performance is reduced. When  
52  
53 operated in parallel however, if the impedances of the MFCs are well matched, then the  
54  
55 internal resistance of the MFC stack will tend towards the lowest common denominator and  
56  
57  
58  
59  
60  
61  
62  
63  
64  
65

1 thus be more uniform [38]. This is evident by the reduction in internal resistance of the  
2 MFC\_S stack from 244 to 76 k $\Omega$ . This large reduction in the internal resistance may also  
3  
4 explain the increase in the current density of the parallel stack from 7.3 mA m<sup>-2</sup> to 18.4 mA  
5  
6 m<sup>-2</sup>, as summarised in Table 1.  
7  
8  
9

10 Considering the results obtained for the MFC\_S stacks, the MFC\_L devices were arranged  
11  
12 only in parallel. As shown in Figure 5B, in this case the maximum power output of the stack  
13  
14 was nearly 6 times higher compared to the MFC\_L individual units. The power density  
15  
16 increased by a factor of 2, and the internal resistance decreased from 33 k $\Omega$  to 1.4 k $\Omega$  (Table  
17  
18  
19  
20 1).  
21  
22

23 The stacking of larger MFCs (mL scale) has been shown to increase the power density of  
24  
25 MFCs, albeit not to the extent observed in this report. For example power densities of  
26  
27 millilitre scale MFCs (6.25 and 12 mL) were improved by a factor of 1.2-1.4 by stacking  
28  
29 multiple units together [21,37]. On the other hand, Aelterman et al. (2006) demonstrates  
30  
31 similar power densities between individual units and MFC stacks when using 60 mL MFCs.  
32  
33  
34  
35  
36  
37  
38  
39  
40  
41  
42  
43  
44  
45  
46  
47  
48  
49  
50  
51  
52  
53  
54  
55  
56  
57  
58  
59  
60  
61  
62  
63  
64  
65

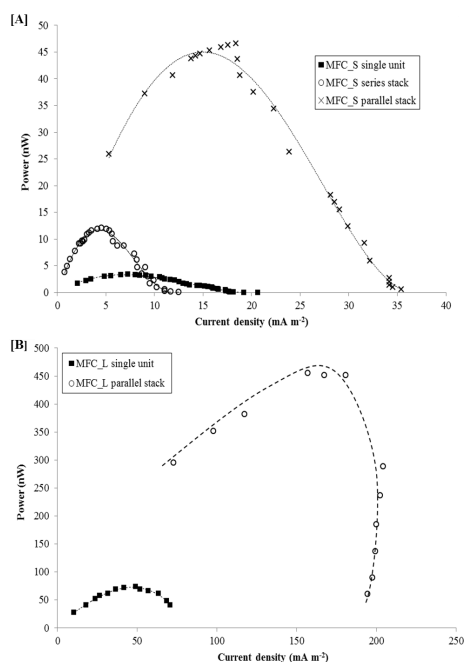


**Figure 5.** Power and polarisation curves. A) Refers to MFC\_S, operated alone, in series and in a parallel stack. Current density refers to the anode surface area, 16 mm<sup>2</sup> for a single unit, 48 mm<sup>2</sup> for the stack. B) Refers to MFC\_L, operated alone and in a parallel stack. Current density refers to the anode surface area, 32 mm<sup>2</sup> for a single unit, 96 mm<sup>2</sup> for the stack.

### 3.3 Use of Biomass-Derived ORR Catalysts

To enhance power generation, without compromising cost-effectiveness and sustainability, two biomass-derived carbon materials, BC1 and BC2, were tested as ORR catalysts at the cathode. Since MFC\_L showed better performance, this study was carried out only on this fuel cell design. The resulting fuel cells were named as MFC\_BC1 and MFC\_BC2 according to the type of catalyst used. Table 1 summarises the results obtained and compares them with the catalyst-free fuel cells previously tested. Figure 6 shows the polarisation and power curves for both devices. The OCV values for MFC\_BC1 and MFC\_BC2 were 151 mV and 220 mV respectively, and thus comparable with MFC\_L.

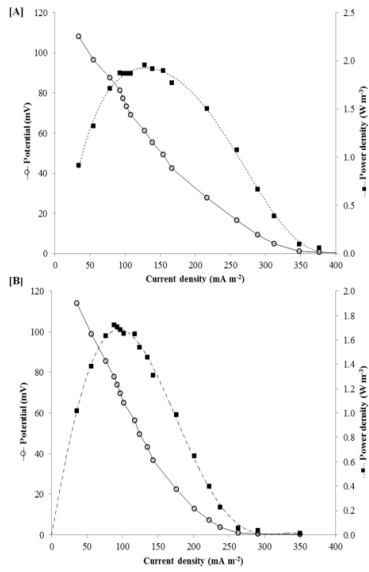


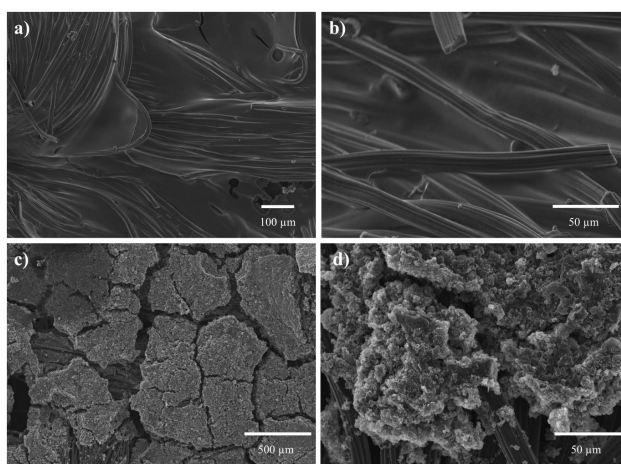
**Figure 6.** Power and polarisation curves. A) refers to MFC\_BC1; B) refers to MFC\_BC2; Current density refers to the anode surface area: MFC\_BC1, MFC\_BC2 = 32 mm<sup>2</sup>. Volumetric power density refers to the MFC chamber volume: MFC\_BC1, MFC\_BC2 = 128 μL. MFC\_BC1 is data from one device, and MFC\_BC2 is an average of two units with 17% error.

As expected, the ORR catalysts enhanced the power performance of the MFCs, leading to a power output and power density almost 3 times higher than MFC\_L. The effectiveness of biomass-derived ORR catalysts may be attributed to the large surface area [17] that the materials exhibit on the cathode surface compared to the plain carbon cloth (BC1: 376 m<sup>2</sup> g<sup>-1</sup>), as well as the capacity of heteroatom doping, such as nitrogen and sulphur, or the incorporation of nanoparticles like iron within the catalyst material to enhance the ORR activity [15,16,40–43].

The internal resistances decreased to values of 15 kΩ and 23 kΩ, for MFC\_BC1 and MFC\_BC2 respectively, down to half those of MFC\_L. Consequently, the current densities were an order of magnitude higher, with a value as high as 127.6 mA m<sup>-2</sup> for MFC\_BC1.

1  
2  
3  
4  
5  
6  
7  
8  
9  
10  
11  
12  
13  
14  
15  
16  
17  
18  
19  
20  
21  
22  
23  
24  
25  
26  
27  
28  
29  
30  
31  
32  
33  
34  
35  
36  
37  
38  
39  
40  
41  
42  
43  
44  
45  
46  
47  
48  
49  
50  
51  
52  
53  
54  
55  
56  
57  
58  
59  
60  
61  
62  
63  
64  
65

Generally MFC\_BC1 performed better, with a 13% higher power density and a 44% increase in current density, compared to MFC\_BC2. The structure of the two doped cathodes may be the reason for this difference. From the SEM images of the doped cathodes (Figure 7), it can be seen that the two ORR catalysts led to very different surface structures. In particular, it appears that BC1 percolated between the carbon fibres of the carbon cloth. Hence, good contact was formed between the carbon fibre electrode and the biomass-derived ORR catalyst, thus allowing a good active surface area for oxygen reduction reactions at the cathode surface. On the other hand, BC2 formed a porous layer on top of the carbon fibres, which have resulted in an added resistance to the system and may explain the poorer performance of MFC\_BC2 with respect to MFC\_BC1.



43  
44  
45  
46  
47  
48  
49  
50  
51  
52  
53  
54  
55  
56  
57  
58  
59  
60  
61  
62  
63  
64  
65

**Figure 7.** SEM images of the two biomass-derived ORR catalyst doped cathode surfaces. a) and b) refer to the cathode used for MFC\_BC1; c) and d) to the case of MFC\_BC2.

**Table 1.** Summary of performance of the several MFCs tested in this study

<b>MFC configuration</b>	<b>OCV (mV)</b>	<b>Internal resistance (k<math>\Omega</math>)</b>	<b>Maximum power output (nW)</b>	<b>Maximum volumetric power density (W m<sup>-3</sup>)</b>	<b>Maximum current density (mA m<sup>-2</sup>)</b>
MFC_S	253	242	3.4	0.053	7.3
MFC_S series stack	151	243	12.1	0.063	4.6
MFC_S parallel stack	206	76	46.7	0.243	18.4
MFC_L	312	33	74.2	0.580	49.1
MFC_L parallel stack	281	1.4	455.1	1.185	157.1
MFC_BC1	151	15	250.1	1.954	127.6
MFC_BC2	220	23	220.1	1.719	88.4

## 4 Conclusions

Microbial fuel cells are an extremely attractive technology for the generation of clean electricity from a range of waste streams. The most viable route to boosting power density generated by MFCs is to develop small scale devices and arrange multiple units in stacks.

In this context, our study aims to guide towards the development of effective miniature MFCs. For this purpose we have developed an innovative miniature MFC, which can easily be further miniaturised. We have used an air-cathode configuration since it has the advantage of greater operational simplicity and cost-effectiveness. While fixing the electrodes spacing to 4 mm, we have investigated the effect of the electrodes length, when the system was continuously fed with artificial urine at a fixed flow rate of  $0.36 \text{ mL min}^{-1}$ .

The doubling of the electrode length of the miniature MFC, and so the hydraulic retention time as well, increased the power density more than tenfold due to enhanced mass transfer properties and substrate consumption at the electrode surface.

By electrically stacking three individual units in parallel, the power output reached the peak value of  $1.2 \text{ W m}^{-3}$ . Moreover, the use of two different types of biomass-derived ORR catalysts at the cathode increased the power density up to threefold. These renewable and cost-effective cathode catalysts are of particular interest for applications in remote or impoverished regions where MFCs could be used for remote and sustainable energy generation from waste.

## Acknowledgements

The authors thank: Wessex Water for providing anaerobic sludge; the Engineering and Physical Sciences Research Council (EPSRC) and the Doctoral Training Centre for Sustainable Chemical Technologies (CSCT) for funding; Stephen Bradley for the SEM images of the doped cathodes. Ioannis Ieropoulos is an EPSRC career acceleration fellow (CAF), grant numbers EP/I004653/1 and EP/L002132/1.

## References

- [1] O. Edenhofer, R. Pichs-Madruga, Y. Sokona, K. Seyboth, P. Matschoss, S. Kadnert, Renewable Energy Sources and Climate Change Mitigation- Special Report of the Intergovernmental Panel on Climate Change, 2011.
- [2] A.P.C. Faaij, Bio-energy in Europe: changing technology choices, *Energy Policy*. 34 (2006) 322–342. doi:10.1016/j.enpol.2004.03.026.
- [3] B. Logan, B. Hamelers, R. Rozendal, U. Schroder, J. Keller, S. Freguia, et al., Critical Review Microbial Fuel Cells : Methodology and Technology, *Environ. Sci. Technol.* 40 (2006) 5181–5192.
- [4] I. Ieropoulos, J. Greenman, C. Melhuish, Urine utilisation by microbial fuel cells; energy fuel for the future., *Phys. Chem. Chem. Phys.* 14 (2012) 94–8. doi:10.1039/c1cp23213d.
- [5] H. Ren, H.-S. Lee, J. Chae, Miniaturizing microbial fuel cells for potential portable power sources: promises and challenges, *Microfluid. Nanofluidics*. 13 (2012) 353–381. doi:10.1007/s10404-012-0986-7.
- [6] K. Rabaey, W. Verstraete, Microbial fuel cells: novel biotechnology for energy generation., *Trends Biotechnol.* 23 (2005) 291–8. doi:10.1016/j.tibtech.2005.04.008.
- [7] H. Liu, B.E. Logan, Electricity generation using an air-cathode single chamber microbial fuel cell in the presence and absence of a proton exchange membrane., *Environ. Sci. Technol.* 38 (2004) 4040–6. <http://www.ncbi.nlm.nih.gov/pubmed/15298217>.
- [8] I. Ieropoulos, P. Ledezma, A. Stinchcombe, G. Papaharalabos, C. Melhuish, J. Greenman, Waste to real energy: the first MFC powered mobile phone., *Phys. Chem. Chem. Phys.* 15 (2013) 15312–6. doi:10.1039/c3cp52889h.



- 1  
2  
3  
4  
5  
6  
7  
8  
9  
10  
11  
12  
13  
14  
15  
16  
17  
18  
19  
20  
21  
22  
23  
24  
25  
26  
27  
28  
29  
30  
31  
32  
33  
34  
35  
36  
37  
38  
39  
40  
41  
42  
43  
44  
45  
46  
47  
48  
49  
50  
51  
52  
53  
54  
55  
56  
57  
58  
59  
60  
61  
62  
63  
64  
65
- [9] S. Choi, Microscale microbial fuel cells: Advances and challenges, *Biosens. Bioelectron.* 69 (2015) 8–25. doi:10.1016/j.bios.2015.02.021.
- [10] A. Baudler, I. Schmidt, M. Langner, A. Greiner, U. Schröder, Does it have to be Carbon? Metal Anodes in Microbial Fuel Cells and related Bioelectrochemical Systems, *Energy Environ. Sci.* (2015). doi:10.1039/C5EE00866B.
- [11] B. Logan, J. Regan, Microbial challenges and applications, *Environ. Sci. Technol.* 40 (2006) 5172–5180. doi:10.1021/es0627592.
- [12] L. Deng, M. Zhou, C. Liu, L. Liu, C. Liu, S. Dong, Development of high performance of Co/Fe/N/CNT nanocatalyst for oxygen reduction in microbial fuel cells., *Talanta.* 81 (2010) 444–8. doi:10.1016/j.talanta.2009.12.022.
- [13] L. Zhang, C. Liu, L. Zhuang, W. Li, S. Zhou, J. Zhang, Manganese dioxide as an alternative cathodic catalyst to platinum in microbial fuel cells., *Biosens. Bioelectron.* 24 (2009) 2825–9. doi:10.1016/j.bios.2009.02.010.
- [14] T. Huggins, H. Wang, J. Kearns, P. Jenkins, Z.J. Ren, Biochar as a sustainable electrode material for electricity production in microbial fuel cells, *Bioresour. Technol.* 157 (2014) 114–119. doi:10.1016/j.biortech.2014.01.058.
- [15] Y. Yuan, T. Yuan, D. Wang, J. Tang, S. Zhou, Sewage sludge biochar as an efficient catalyst for oxygen reduction reaction in an microbial fuel cell, *Bioresour. Technol.* 144 (2013) 115–120. doi:10.1016/j.biortech.2013.06.075.
- [16] H. Yuan, L. Deng, Y. Qi, N. Kobayashi, J. Tang, Nonactivated and Activated Biochar Derived from Bananas as Alternative Cathode Catalyst in Microbial Fuel Cells, *Sci. World J.* 2014 (2014).
- [17] S.-A. Wohlgemuth, R.J. White, M.-G. Willinger, M.-M. Titirici, M. Antonietti, A one-pot hydrothermal synthesis of sulfur and nitrogen doped carbon aerogels with enhanced electrocatalytic activity in the oxygen reduction reaction, *Green Chem.* 14 (2012) 1515. doi:10.1039/c2gc35309a.
- [18] M. Li, Y. Xiong, X. Liu, C. Han, Y. Zhang, X. Bo, et al., Iron and nitrogen co-doped carbon nanotube@hollow carbon fibers derived from plant biomass as efficient catalysts for the oxygen reduction reaction, *J. Mater. Chem. A.* 3 (2015) 9658–9667. doi:10.1039/C5TA00958H.
- [19] T.H. Pham, K. Rabaey, P. Aelterman, P. Clauwaert, L. De Schampelaire, N. Boon, et al., Microbial Fuel Cells in Relation to Conventional Anaerobic Digestion Technology, *Eng. Life Sci.* 6 (2006) 285–292. doi:10.1002/elsc.200620121.
- [20] L. Woodward, M. Perrier, B. Srinivasan, C. Hc, B. Tartakovsky, Maximizing Power Production in a Stack of Microbial Fuel Cells Using Multiunit Optimization Method, *Biotechnol. Prog.* 25 (2009) 676–682. doi:10.1021/bp.115.

- 1 [21] I. Ieropoulos, J. Greenman, C. Melhuish, Miniature microbial fuel cells and stacks for  
2 urine utilisation, *Int. J. Hydrogen Energy*. 38 (2013) 492–496.  
3 doi:10.1016/j.ijhydene.2012.09.062.
- 4 [22] F. Qian, D.E. Morse, Miniaturizing microbial fuel cells., *Trends Biotechnol.* 29 (2011)  
5 62–9. doi:10.1016/j.tibtech.2010.10.003.
- 6 [23] F. Qian, Z. He, M.P. Thelen, Y. Li, A microfluidic microbial fuel cell fabricated by soft  
7 lithography., *Bioresour. Technol.* 102 (2011) 5836–40.  
8 doi:10.1016/j.biortech.2011.02.095.
- 9 [24] T. Brooks, C.W. Keevil, A simple artificial urine for the growth of urinary pathogens.,  
10 *Lett. Appl. Microbiol.* 24 (1997) 203–6.  
11 <http://www.ncbi.nlm.nih.gov/pubmed/9080700>.
- 12 [25] R.J. White, N. Yoshizawa, M. Antonietti, M.-M. Titirici, A sustainable synthesis of  
13 nitrogen-doped carbon aerogels, *Green Chem.* 13 (2011) 2428.  
14 doi:10.1039/c1gc15349h.
- 15 [26] H. Ren, C.I. Torres, P. Parameswaran, B.E. Rittmann, J. Chae, Improved current and  
16 power density with a micro-scale microbial fuel cell due to a small characteristic  
17 length., *Biosens. Bioelectron.* 61 (2014) 587–92. doi:10.1016/j.bios.2014.05.037.
- 18 [27] T.K. Sherwood, R.L. Pigford, C.R. Wilke, *Mass Transfer*, McGraw-Hill, New York,  
19 1975.
- 20 [28] S. Choi, H.-S. Lee, Y. Yang, P. Parameswaran, C.I. Torres, B.E. Rittmann, et al., A  
21  $\mu\text{L}$ -scale micromachined microbial fuel cell having high power density., *Lab Chip.* 11  
22 (2011) 1110–7. doi:10.1039/c0lc00494d.
- 23 [29] F. Qian, M. Baum, Q. Gu, D.E. Morse, A 1.5 microL microbial fuel cell for on-chip  
24 bioelectricity generation., *Lab Chip.* 9 (2009) 3076–81. doi:10.1039/b910586g.
- 25 [30] A. Elmekawy, H.M. Hegab, X. Dominguez-Benetton, D. Pant, Internal resistance of  
26 microfluidic microbial fuel cell: challenges and potential opportunities., *Bioresour.*  
27 *Technol.* 142 (2013) 672–82. doi:10.1016/j.biortech.2013.05.061.
- 28 [31] H.-Y. Wang, A. Bernarda, C.-Y. Huang, D.-J. Lee, J.-S. Chang, Micro-sized microbial  
29 fuel cell: a mini-review., *Bioresour. Technol.* 102 (2011) 235–43.  
30 doi:10.1016/j.biortech.2010.07.007.
- 31 [32] B. Inman, W. Etienne, R. Rubin, R. Owusu, T. Oliveira, D. Rodrigues, et al., The  
32 impact of temperature and urinary constituents on urine viscosity and its relevance to  
33 bladder hyperthermia treatment, *Int. J. Hyperth.* 29 (2013) 206–210.  
34 doi:10.3109/02656736.2013.775355.
- 35 [33] B.Y. Louis, D. Akeley, A Study of the Diffusion of Urea in Water at 25 C with the  
36 Gouy Interference Method, *J. Am. Chem. Soc.* 74 (1952) 2058–2060.  
37 doi:10.1021/ja01128a060.
- 38  
39  
40  
41  
42  
43  
44  
45  
46  
47  
48  
49  
50  
51  
52  
53  
54  
55  
56  
57  
58  
59  
60  
61  
62  
63  
64  
65

- 1  
2  
3  
4  
5  
6  
7  
8  
9  
10  
11  
12  
13  
14  
15  
16  
17  
18  
19  
20  
21  
22  
23  
24  
25  
26  
27  
28  
29  
30  
31  
32  
33  
34  
35  
36  
37  
38  
39  
40  
41  
42  
43  
44  
45  
46  
47  
48  
49  
50  
51  
52  
53  
54  
55  
56  
57  
58  
59  
60  
61  
62  
63  
64  
65
- [34] J. Lee, K.G. Lim, G.T.R. Palmore, A. Tripathi, Optimization of microfluidic fuel cells using transport principles., *Anal. Chem.* 79 (2007) 7301–7. doi:10.1021/ac070812e.
- [35] C. Liu, J. Li, X. Zhu, L. Zhang, D. Ye, R.K. Brown, et al., Effects of brush lengths and fiber loadings on the performance of microbial fuel cells using graphite fiber brush anodes, *Int. J. Hydrogen Energy.* 38 (2013) 15646–15652. doi:10.1016/j.ijhydene.2013.03.144.
- [36] I. Ieropoulos, J. Greenman, C. Melhuish, Improved energy output levels from small-scale Microbial Fuel Cells., *Bioelectrochemistry.* 78 (2010) 44–50. doi:10.1016/j.bioelechem.2009.05.009.
- [37] P. Ledezma, J. Greenman, I. Ieropoulos, MFC-cascade stacks maximise COD reduction and avoid voltage reversal under adverse conditions., *Bioresour. Technol.* 134 (2013) 158–65. doi:10.1016/j.biortech.2013.01.119.
- [38] G. Papaharalabos, J. Greenman, C. Melhuish, I. Ieropoulos, A novel small scale Microbial Fuel Cell design for increased electricity generation and waste water treatment, *Int. J. Hydrogen Energy.* 40 (2015) 4263–4268. doi:10.1016/j.ijhydene.2015.01.117.
- [39] P. Aelterman, K. Rabaey, H.T. Pham, N. Boon, W. Verstraete, Continuous Electricity Generation at High Voltages and Currents Using Stacked Microbial Fuel Cells, *Environ. Sci. Technol.* 40 (2006) 3388–3394. doi:10.1021/es0525511.
- [40] J. Liu, P. Song, Z. Ning, W. Xu, Recent Advances in Heteroatom-Doped Metal-Free Electrocatalysts for Highly Efficient Oxygen Reduction Reaction, *Electrocatalysis.* 6 (2015) 132–147. doi:10.1007/s12678-014-0243-9.
- [41] N. Daems, X. Sheng, I.F.J. Vankelecom, P.P. Pescarmona, Metal-free doped carbon materials as electrocatalysts for the oxygen reduction reaction, *J. Mater. Chem. A.* 2 (2014) 4085–4110. doi:10.1039/C3TA14043A.
- [42] F. Charreteur, F. Jaouen, S. Ruggeri, J.-P. Dodelet, Fe/N/C non-precious catalysts for PEM fuel cells: Influence of the structural parameters of pristine commercial carbon blacks on their activity for oxygen reduction, *Electrochim. Acta.* 53 (2008) 2925–2938. doi:10.1016/j.electacta.2007.11.002.
- [43] U.I. Kramm, J. Herranz, N. Larouche, T.M. Arruda, M. Lefèvre, F. Jaouen, et al., Structure of the catalytic sites in Fe/N/C-catalysts for O<sub>2</sub>-reduction in PEM fuel cells., *Phys. Chem. Chem. Phys.* 14 (2012) 11673–88. doi:10.1039/c2cp41957b.

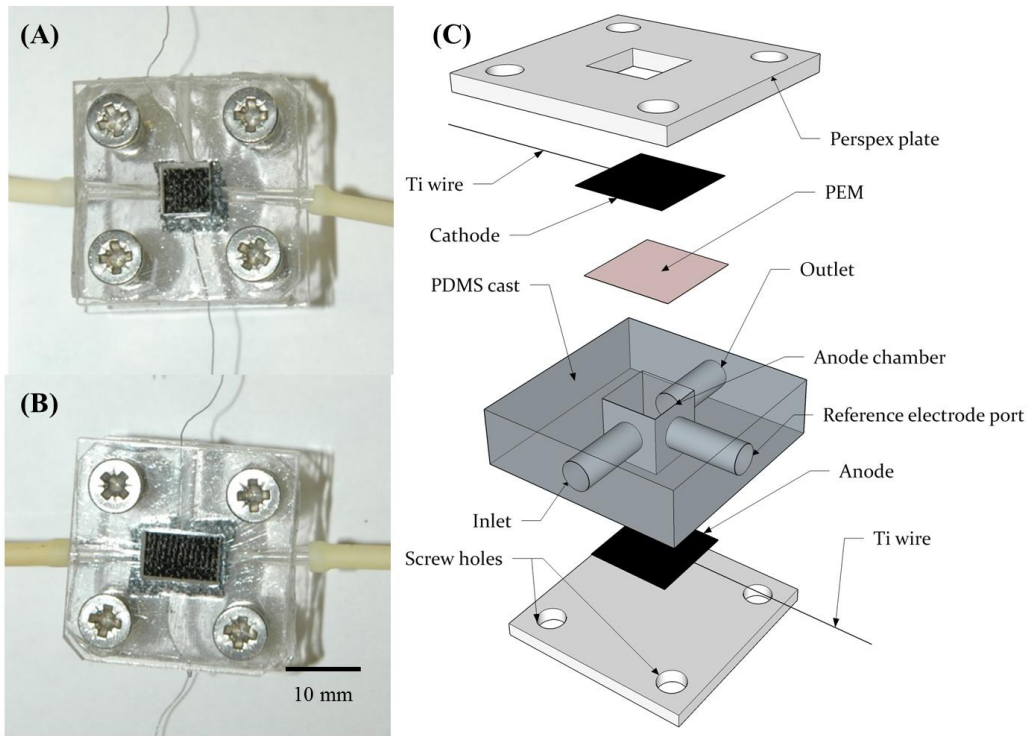


**Figure 1.** MFCs used in this study; A: Photograph of MFC\_S; B: Photograph of MFC\_L; C: Schematic layout of the device.

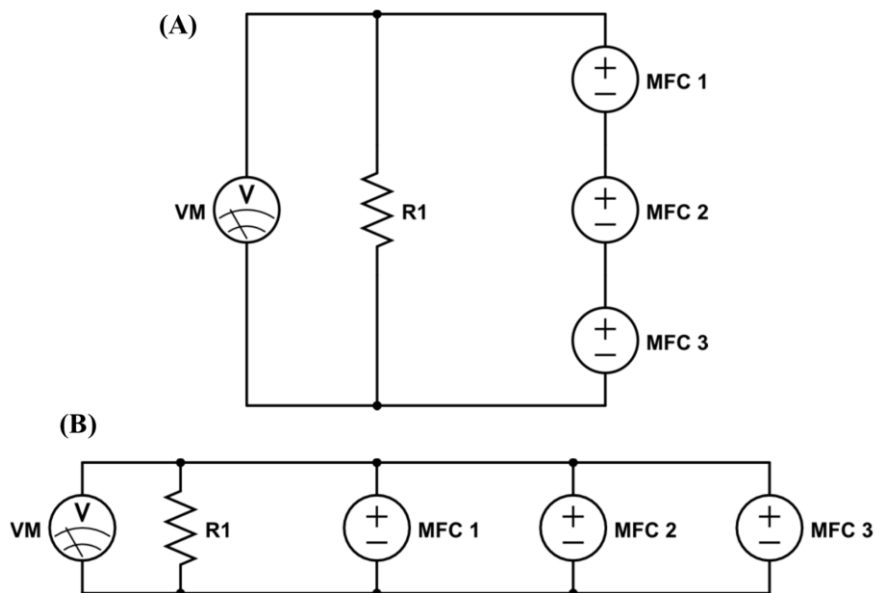


**Figure 2.** Schematic for electrical stacking MFC units in series (A) and in parallel (B): R1 = external load, VM = voltmeter.

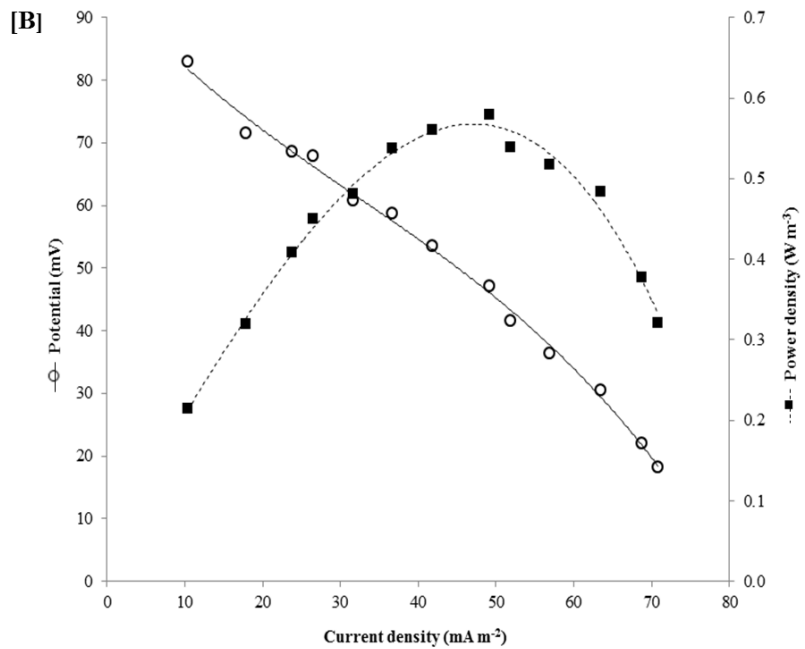
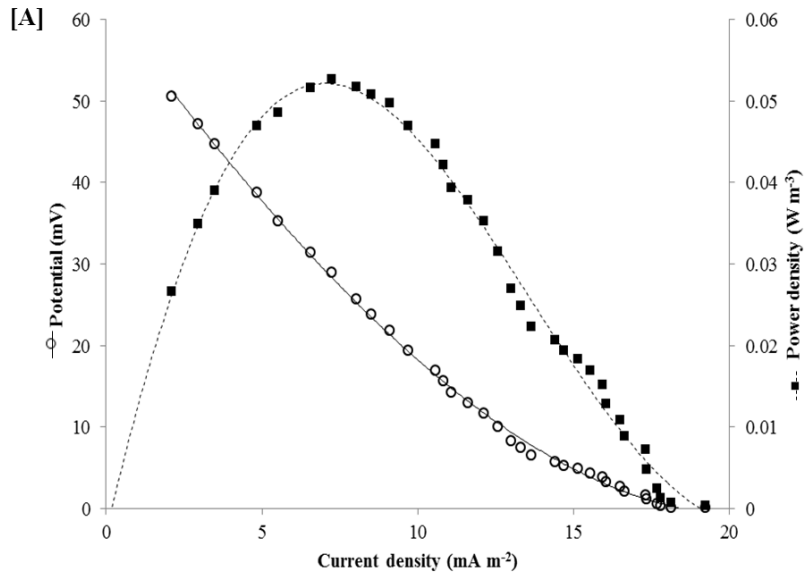


**Figure 3.** Power and polarisation curves. A: MFC\_S; B: MFC\_L. Current density refers to the anode surface area: MFC\_S = 16 mm<sup>2</sup>; MFC\_L = 32 mm<sup>2</sup>. Volumetric power density refers to the MFC chamber volume: MFC\_S = 64 μL; MFC\_L = 128 μL. For each geometry, data is the average of 3 devices, with up to 22% error.

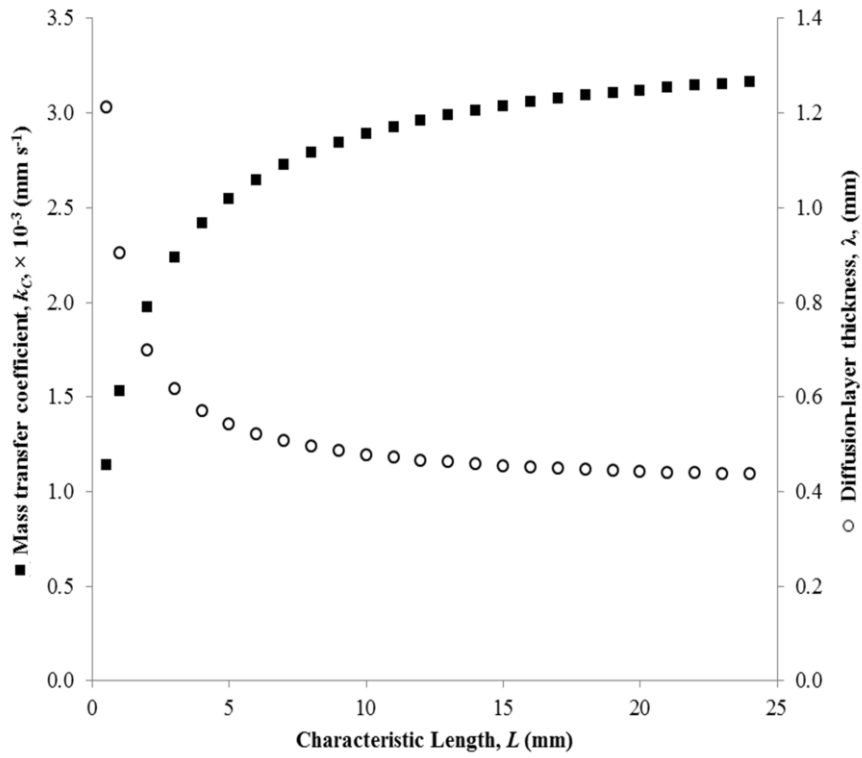


**Figure 4.** Effect of length of MFC channel on mass transfer coefficient and diffusion-layer thickness moving from 0.5 to 25 mm. Values plotted are for a flow rate of 0.36 mL min<sup>-1</sup>.

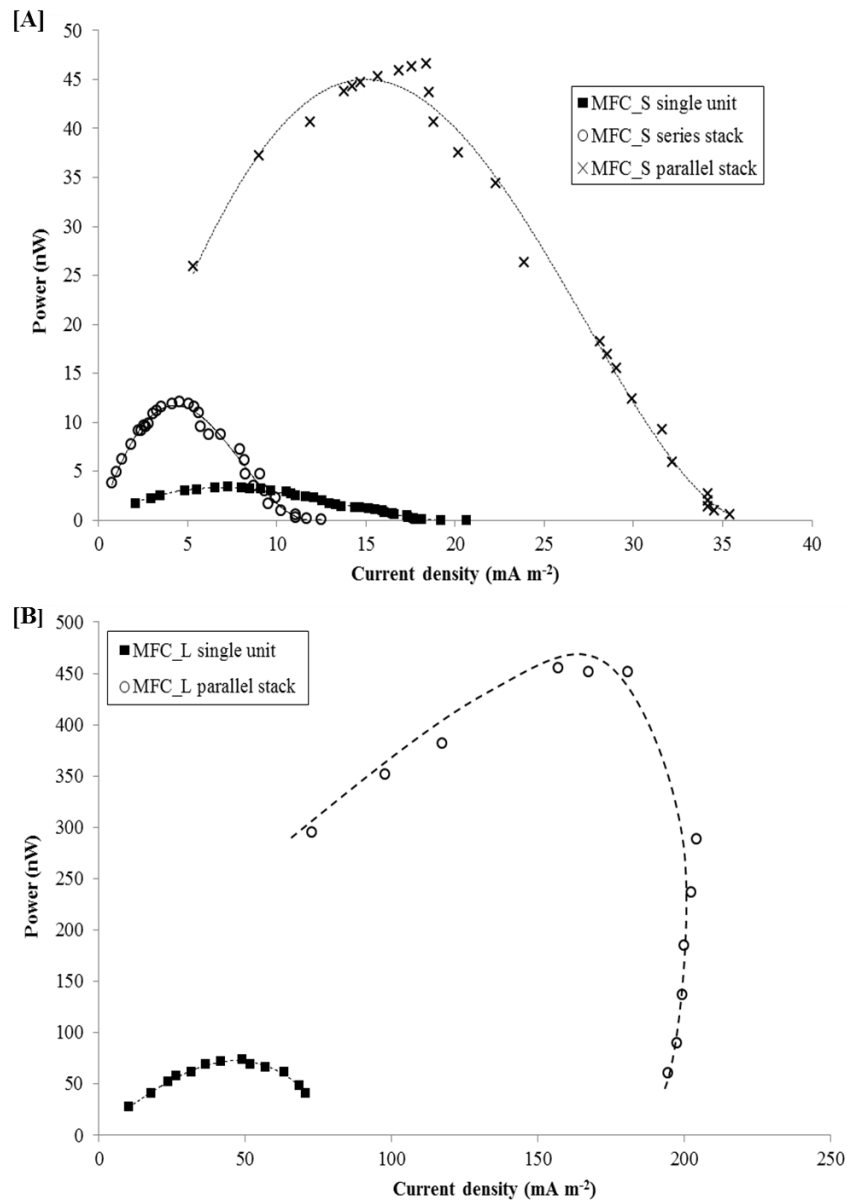


**Figure 5.** Power and polarisation curves. A) Refers to MFC\_S, operated alone, in series and in a parallel stack. Current density refers to the anode surface area, 16 mm<sup>2</sup> for a single unit, 48 mm<sup>2</sup> for the stack. B) Refers to MFC\_L, operated alone and in a parallel stack. Current density refers to the anode surface area, 32 mm<sup>2</sup> for a single unit, 96 mm<sup>2</sup> for the stack.

1  
2  
3  
4  
5  
6  
7  
8  
9  
10  
11  
12  
13  
14  
15  
16  
17  
18  
19  
20  
21  
22  
23  
24  
25  
26  
27  
28  
29  
30  
31  
32  
33  
34  
35  
36  
37  
38  
39  
40  
41  
42  
43  
44  
45  
46  
47  
48  
49  
50  
51  
52  
53  
54  
55  
56  
57  
58  
59  
60  
61  
62  
63  
64  
65

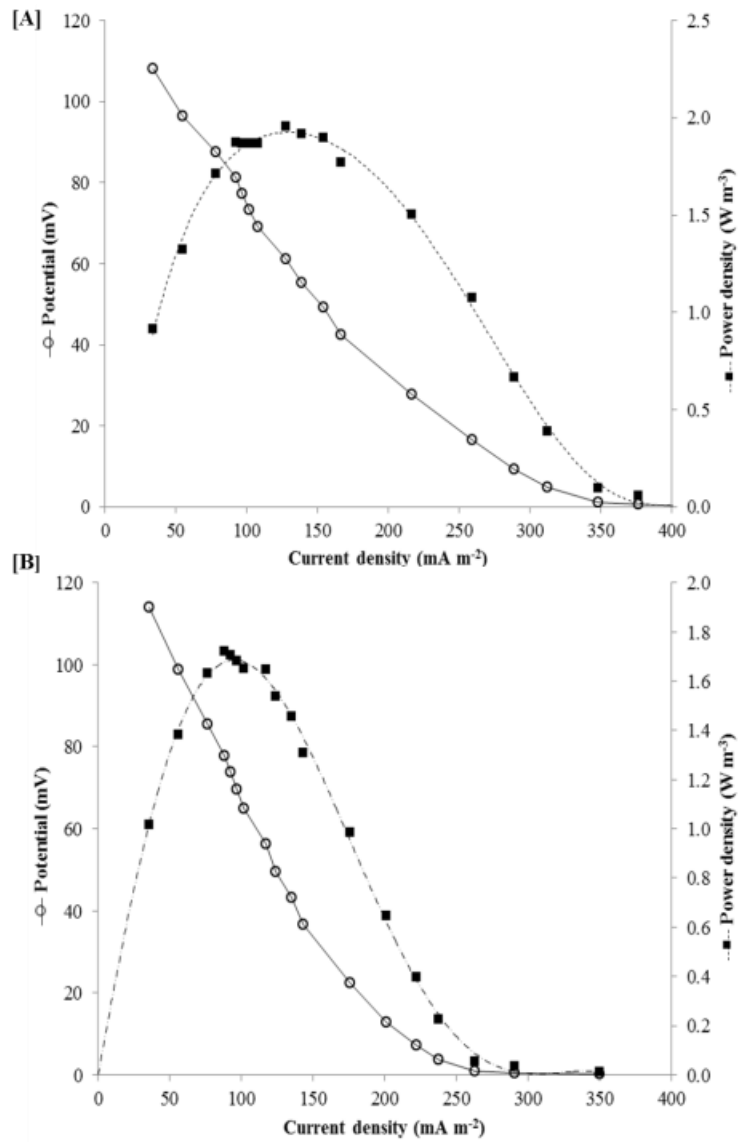


**Figure 6.** Power and polarisation curves. A) refers to MFC\_BC1; B) refers to MFC\_BC2; Current density refers to the anode surface area: MFC\_BC1, MFC\_BC2 = 32 mm<sup>2</sup>. Volumetric power density refers to the MFC chamber volume: MFC\_BC1, MFC\_BC2 = 128  $\mu$ L. MFC\_BC1 is data from one device, and MFC\_BC2 is an average of two units with 17% error.



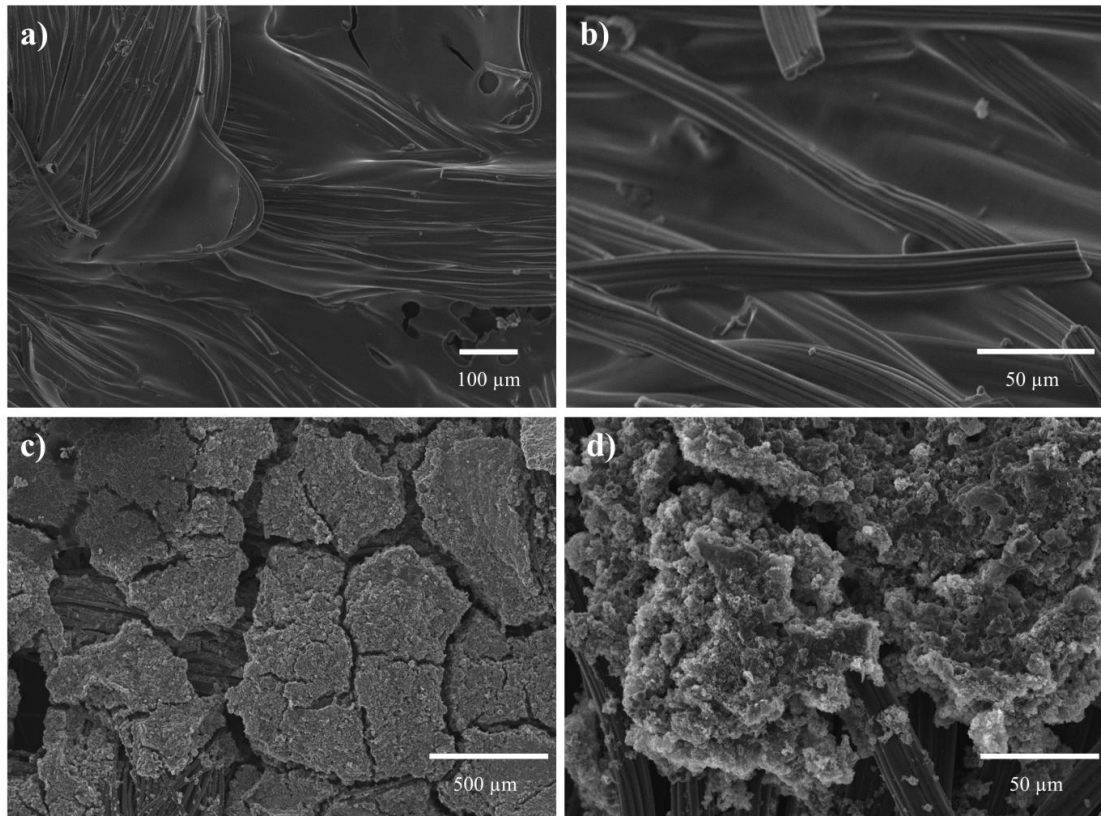


**Figure 7.** SEM images of the two biomass-derived ORR catalyst doped cathode surfaces. a) and b) refer to the cathode used for MFC\_BC1; c) and d) to the case of MFC\_BC2.

**Table 1.** Summary of performance of the several MFCs tested in this study

<b>MFC configuration</b>	<b>OCV (mV)</b>	<b>Internal resistance (k<math>\Omega</math>)</b>	<b>Maximum power output (nW)</b>	<b>Maximum volumetric power density (W m<sup>-3</sup>)</b>	<b>Maximum current density (mA m<sup>-2</sup>)</b>
MFC_S	253	242	3.4	0.053	7.3
MFC_S series stack	151	243	12.1	0.063	4.6
MFC_S parallel stack	206	76	46.7	0.243	18.4
MFC_L	312	33	74.2	0.580	49.1
MFC_L parallel stack	281	1.4	455.1	1.185	157.1
MFC_BC1	151	15	250.1	1.954	127.6
MFC_BC2	220	23	220.1	1.719	88.4

Figure 1  
[Click here to download high resolution image](#)

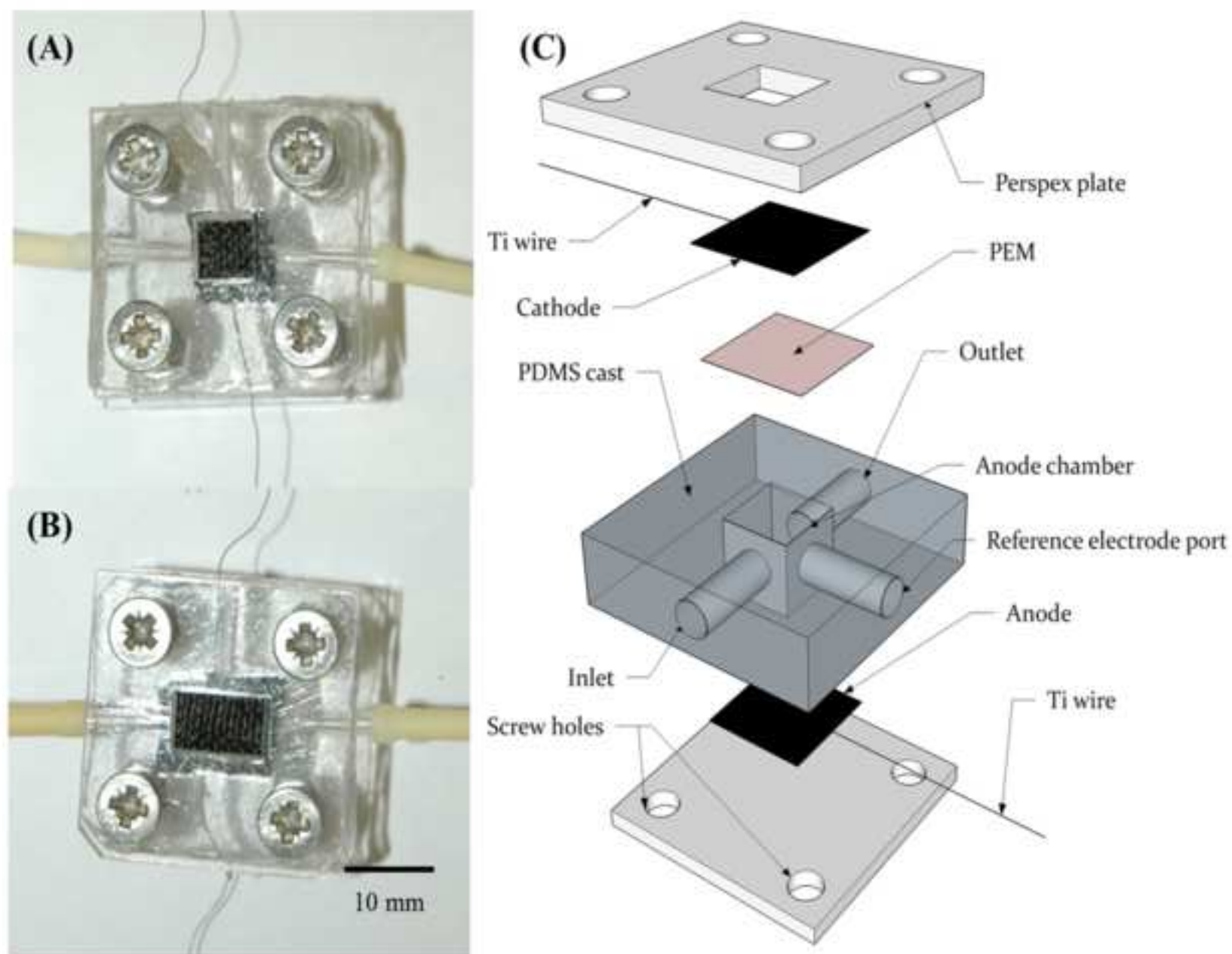


Figure 2  
[Click here to download high resolution image](#)

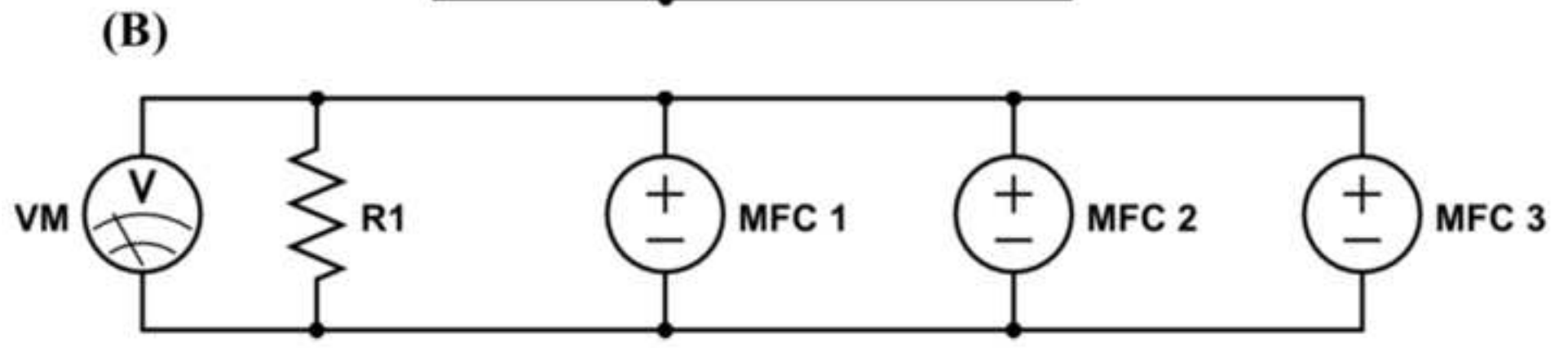
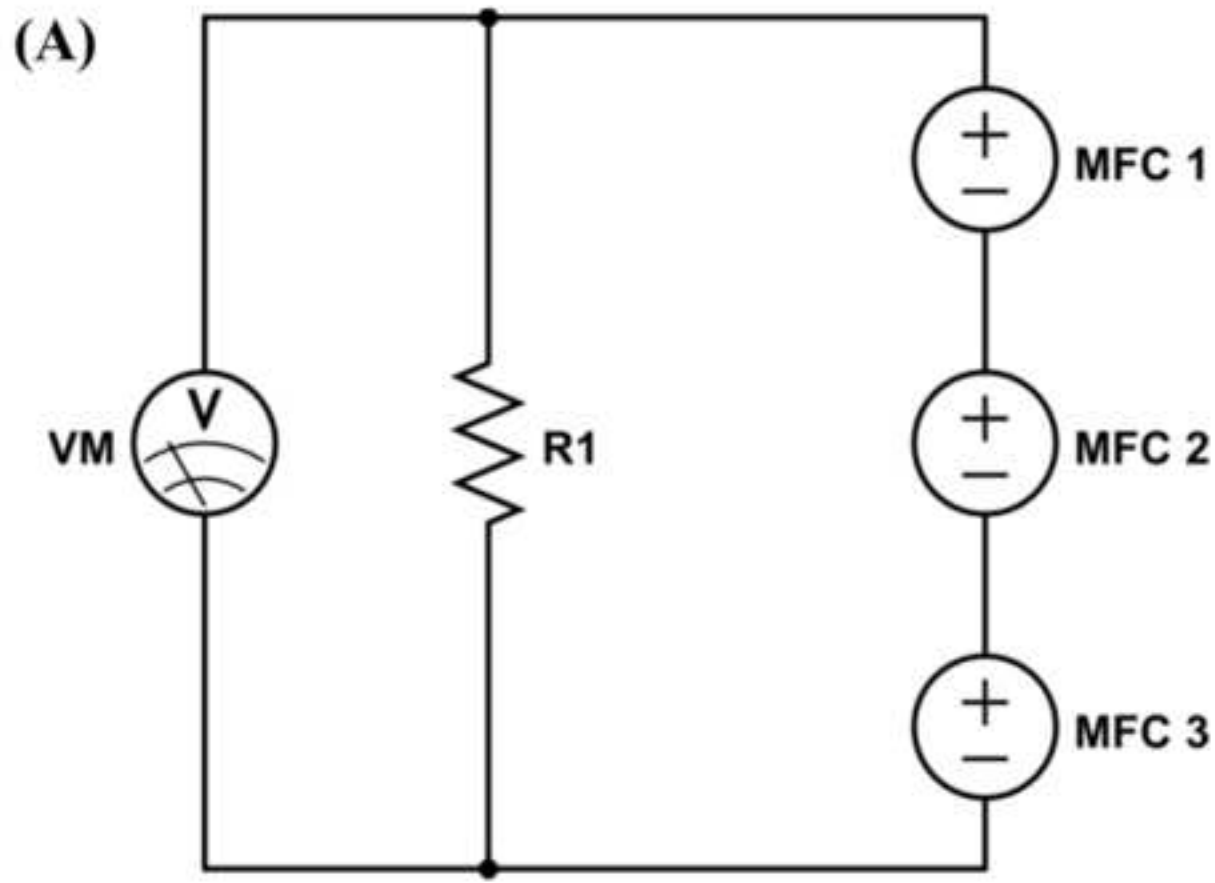


Figure 3  
[Click here to download high resolution image](#)

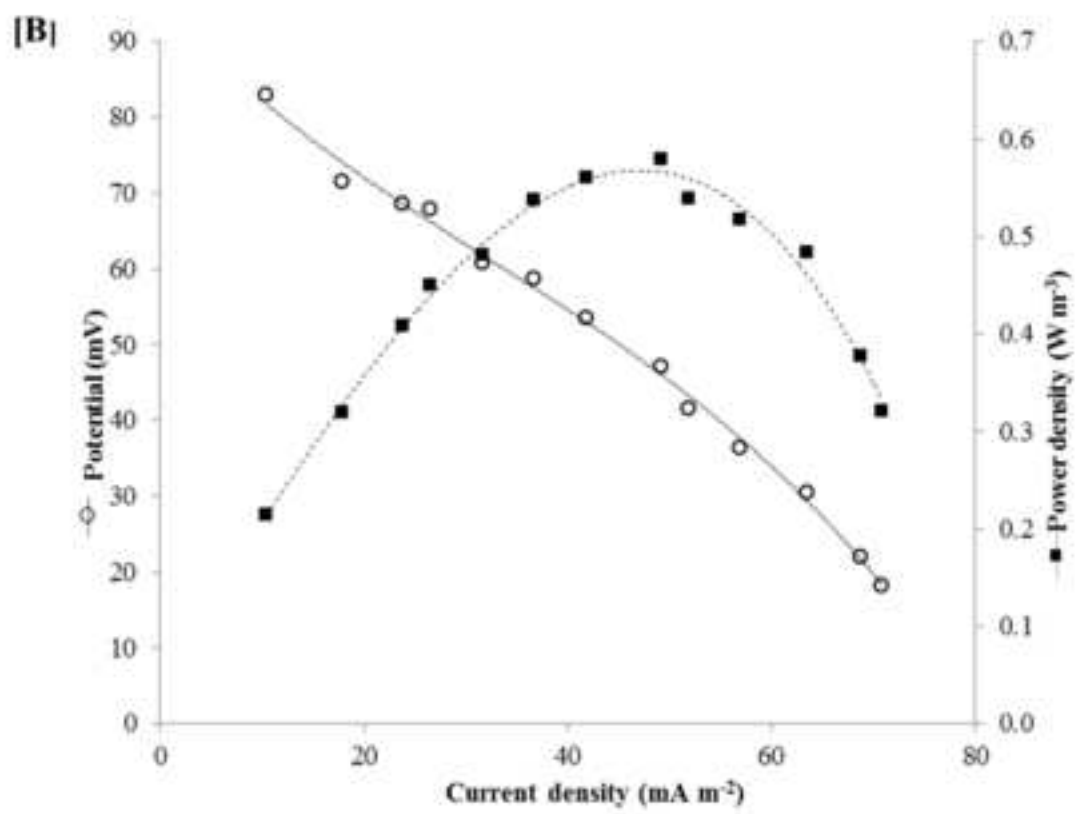
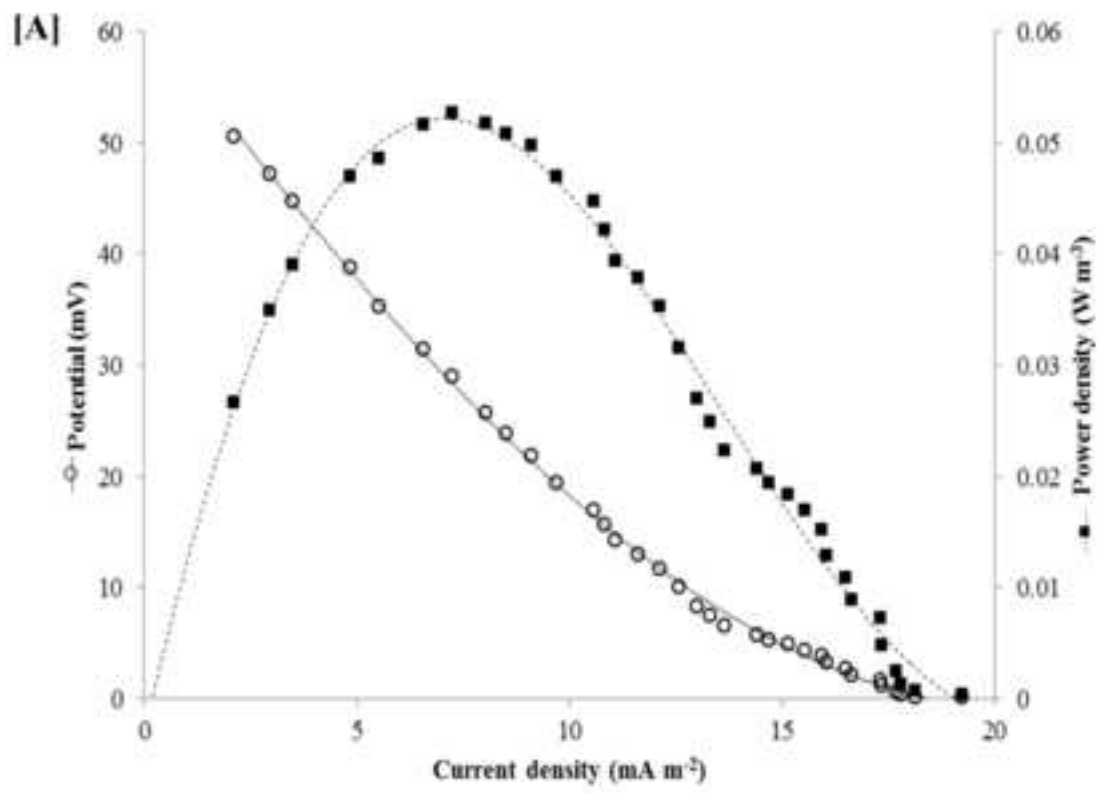


Figure 4  
[Click here to download high resolution image](#)

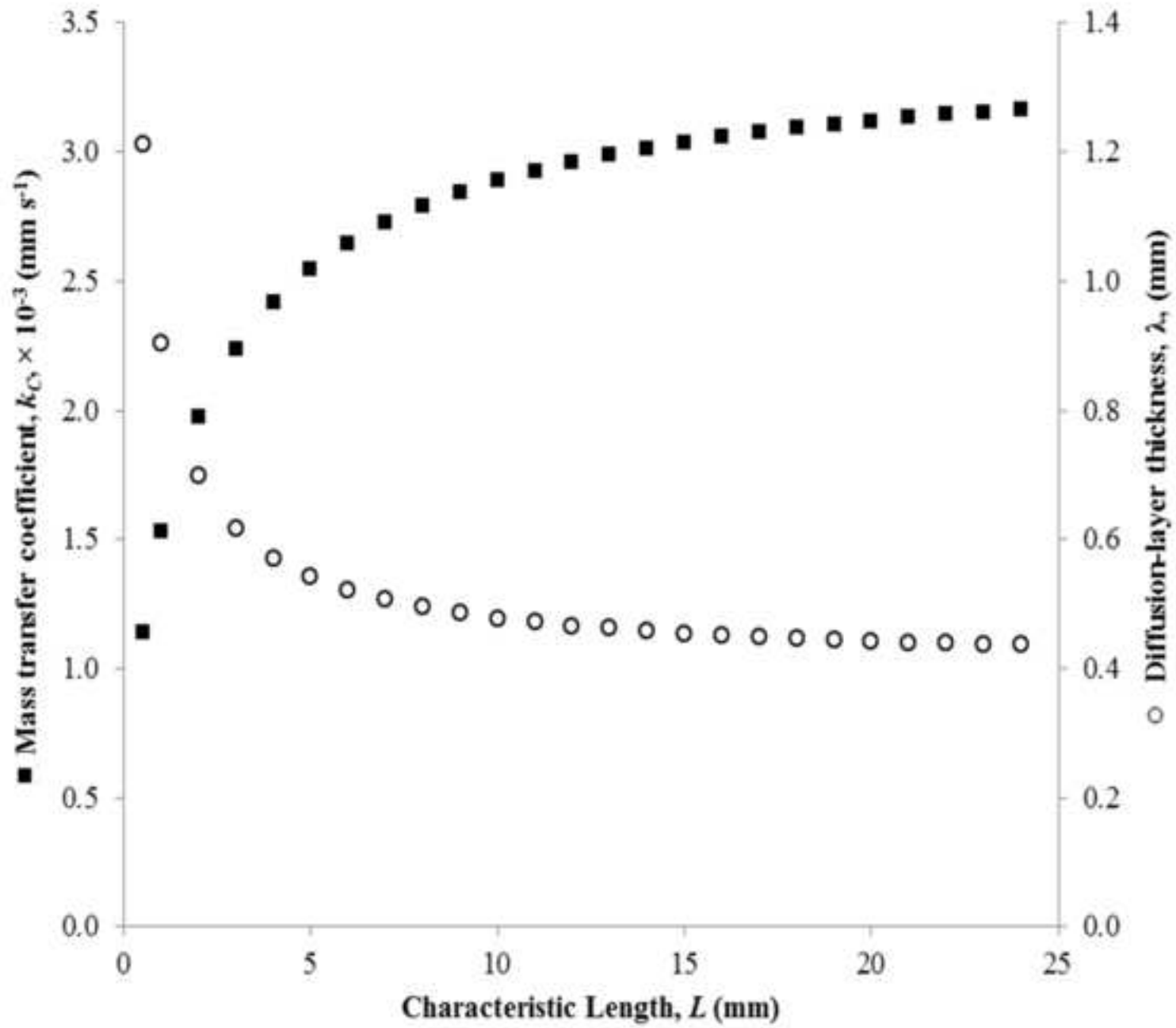


Figure 5  
[Click here to download high resolution image](#)

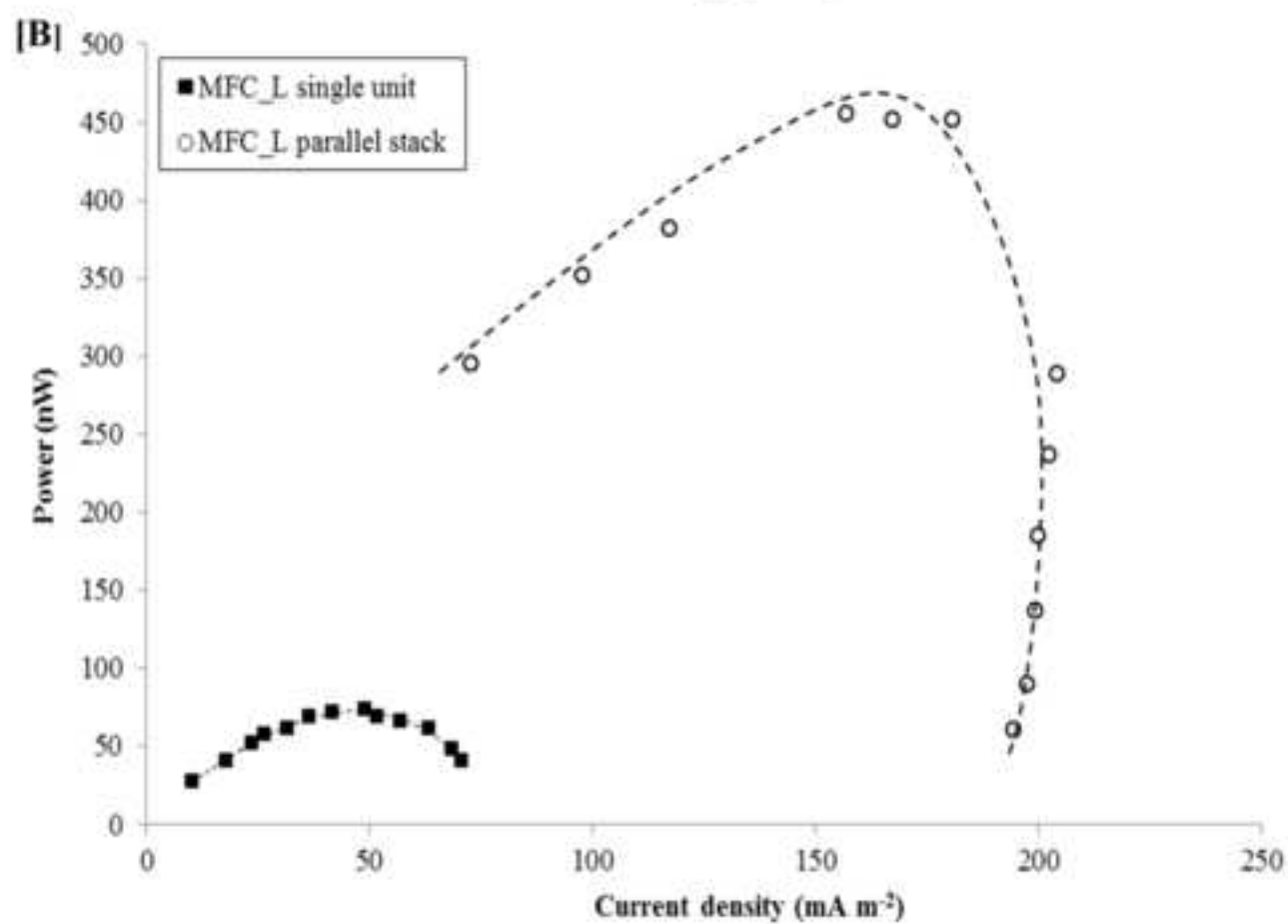
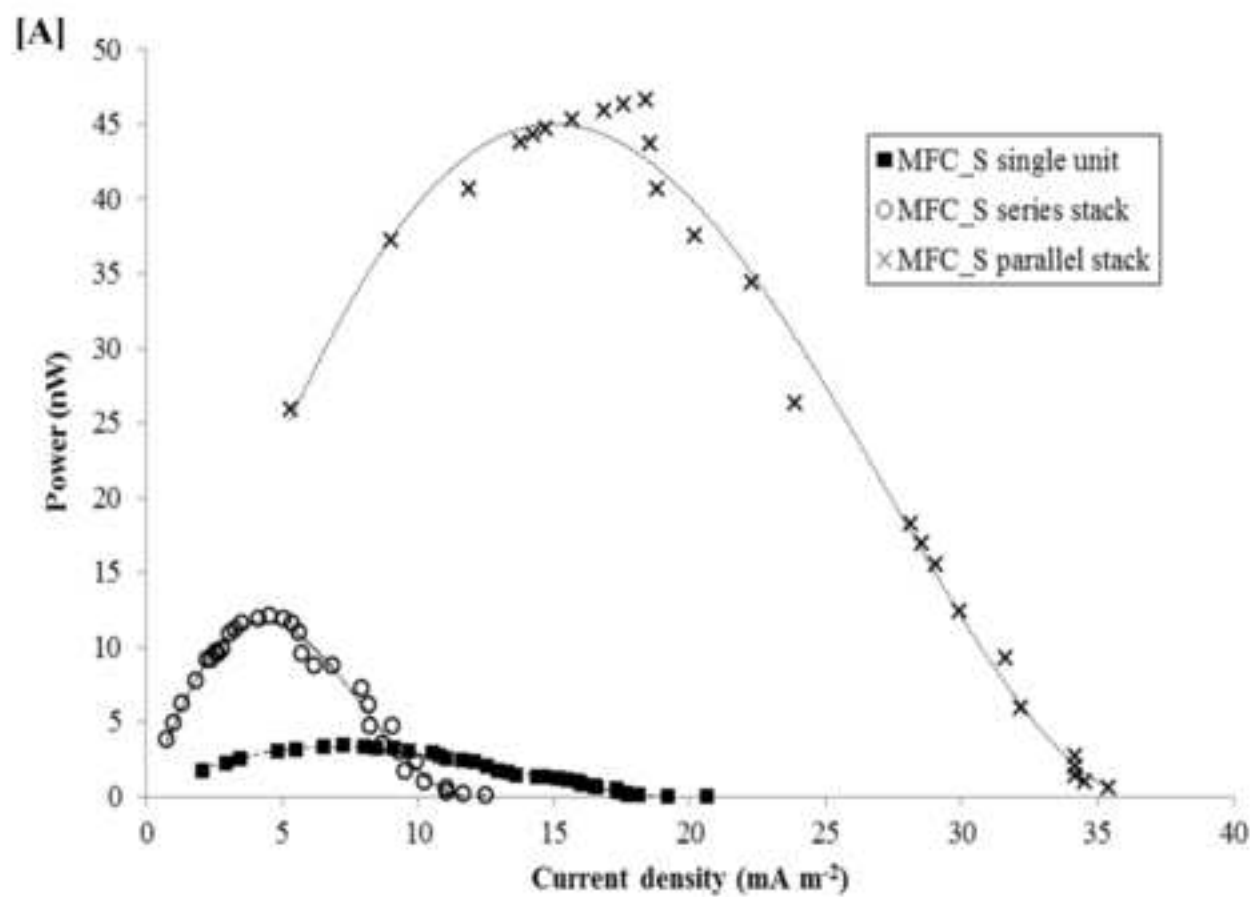


Figure 6

[Click here to download high resolution image](#)

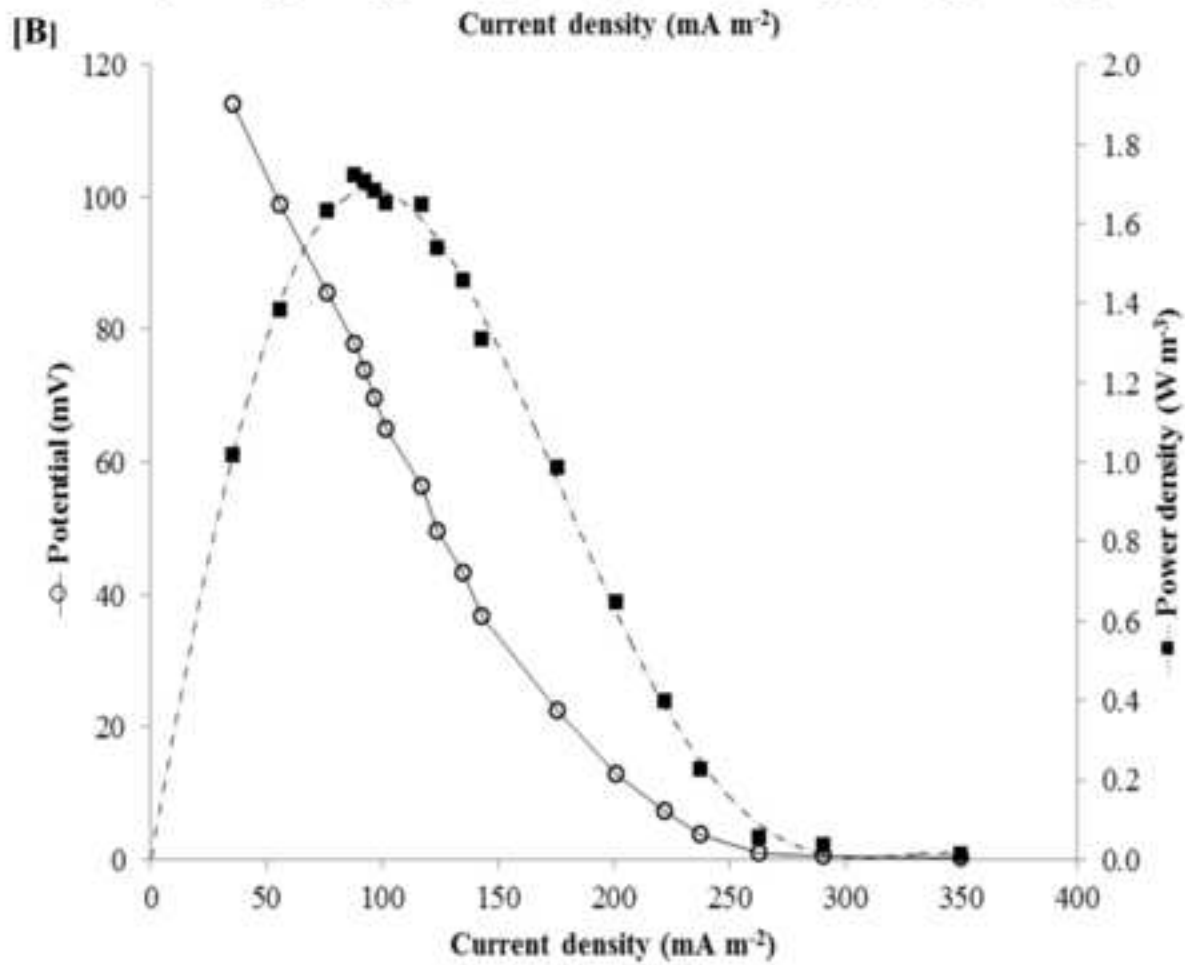
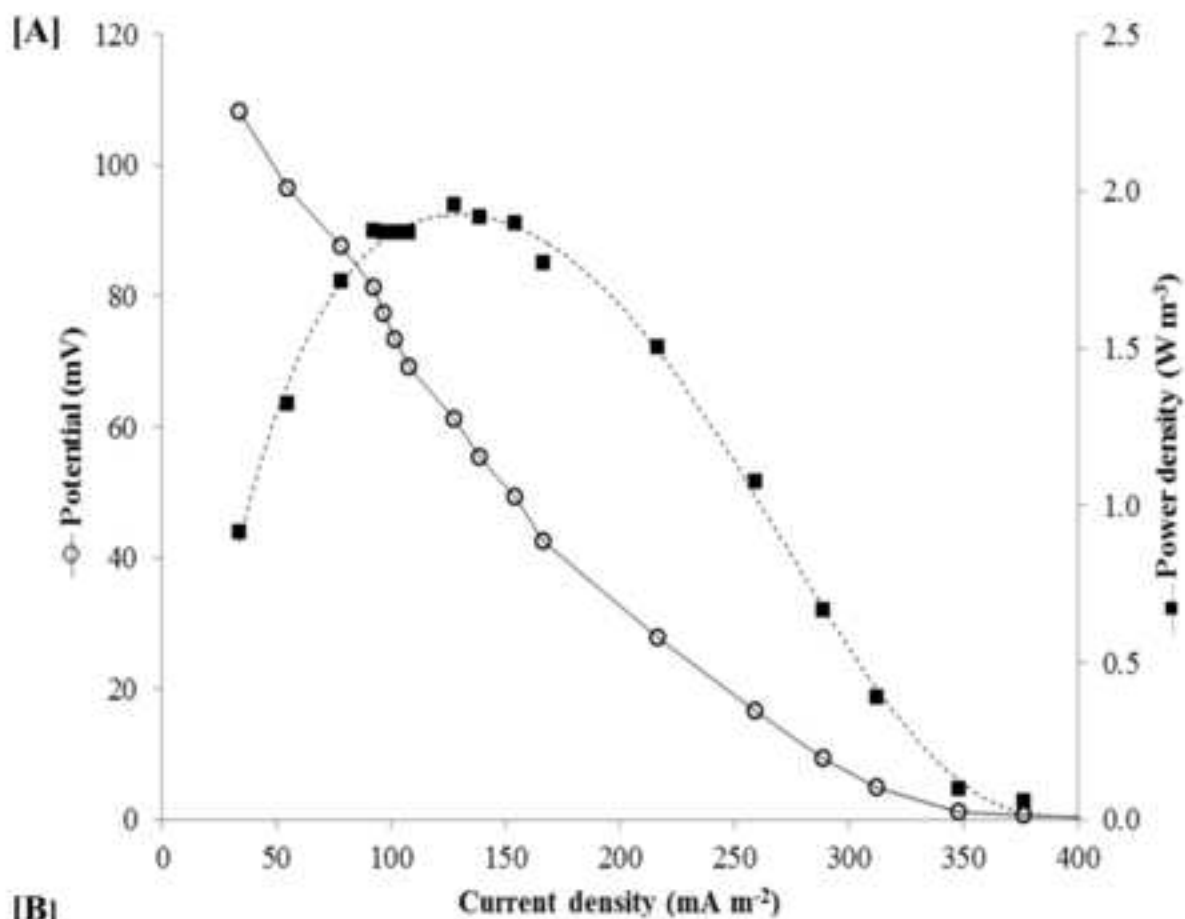




Figure 7  
[Click here to download high resolution image](#)

